Interaction of Mithramycin and Chromomycin A_3 with d(TAGCTAGCTA)$_2$: Role of Sugars in Antibiotic−DNA Recognition[||]

Sukanya Chakrabarti,[†,‡] Bhabatarak Bhattacharyya,[§] and Dipak Dasgupta*[,†]

Biophysics Division, Saha Institute of Nuclear Physics, 37 Belgachhia Road, Kolkata 700 037, India, and Department of Biochemistry, Bose Institute, P1/12 CIT Scheme VIIM, Kolkata 700 054, India

Received: December 31, 2001; In Final Form: March 19, 2002

The anticancer antibiotics mithramycin (MTR) and chromomycin A_3 (CHR) inhibit macromolecular biosynthesis by binding reversibly to double-stranded DNA via the minor groove with GC base specificity in the presence of divalent cations such as Mg^{2+}. They have different saccharide residues. Here, the role of the sugars in DNA recognition by the antibiotics has been investigated by use of a model oligomer, d(TAGCTAGCTA)$_2$, that contains two partially overlapping potential binding sites (GpC). Spectroscopic studies along with analysis of binding and thermodynamic parameters for the interaction(s) of the antibiotics with the oligomer illustrate that $(MTR)_2Mg^{2+}$ binds with a 2:1 stoichiometry in contrast to a 1:1 stoichiometry for $(CHR)_2Mg^{2+}$, in terms of ligand:duplex. Both associations are enthalpy-driven, the enthalpy change being higher in the case of $(MTR)_2Mg^{2+}$. Analysis of melting profiles of the oligomer in the absence and presence of the two ligands show that $(MTR)_2Mg^{2+}$ stabilizes the duplex. On the other hand, $(CHR)_2Mg^{2+}$ stabilizes only half of the oligomer and destabilizes the other part. This is concluded from the appearance of two peaks in the differential melting curve, where the first peak is below the melting temperature of free oligomer and the second peak is above it. The experimental results lead to the following conclusions regarding the role of the sugars. The presence of substituents such as methoxy and acetoxy groups in the A, B, and E sugars of CHR reduces the flexibility of $(CHR)_2Mg^{2+}$ ligand. As a consequence, its association with the first binding site in the oligomer leads to partial unwinding and destabilization of the second site. Hence, $(CHR)_2Mg^{2+}$ is unable to interact with both sites in the oligomer. In contrast, $(MTR)_2Mg^{2+}$ is more flexible. It undergoes conformational changes leading to 2:1 binding stoichiometry with the oligomer. Thus, the nature of substituents in the saccharides is a major factor leading to difference in DNA recognition properties of the antibiotics.

Introduction

Mithramycin (MTR) and chromomycin A_3 (CHR) (Figure 1) are two anticancer antibiotics belonging to the aureolic acid group. They inhibit DNA transcription and replication in vivo[2,3] by binding reversibly to template DNA in the minor groove with GC base specificity.[4−7] At and above physiological pH, the association takes place only in the presence of divalent cations[5] like Mg^{2+}. It was shown from our laboratory for the first time that, in the absence of DNA, antibiotics bind Mg^{2+} to form two different types of antibiotic−Mg^{2+} complexes: complex I (1:1) and complex II (2:1) in terms of antibiotic: Mg^{2+} with different stability constants. The two complexes are different molecular entities as shown by spectroscopic and kinetic studies supported by HPLC characterization.[8−12] They are the potential DNA binding ligands and bind DNA differently.[9,11−15]

The antibiotics are structurally related. Each consists of a planar aglycon, the chromomycinone moiety, with a disaccharide and a trisaccharide linked on either side (Figure 1). They differ in their sugar residues. Also, MTR does not contain acetoxy or methoxy substituents on its sugar residues. The differences lead to significant dissimilarities in the physicochemical properties: MTR has a pK_a of 5.0, but CHR has a pK_a of 7.0.[16]

Gross structural similarities between the two antibiotics lead to GC base-specific association for the antibiotic−Mg^{2+} complex-(es) with DNA. Base specificity has been ascribed to the hydrogen bonds formed between potential sites in the guanine base and ligand(s).[13−15] In a previous study of complex II−polynucleotide interaction, we have shown that accessibility of the 2-amino functional group in the guanine base depends on the size of the minor groove.[17] Therefore, widening of the deep and narrow B-DNA minor groove to an A-type conformation is necessary for the association of the $(antibiotic)_2Mg^{2+}$ ligand-(s).[13,15,17,18]

A closer scrutiny of DNA binding properties has also indicated the role played by sugar moieties of the antibiotics. Comparison of thermodynamic parameters associated with the interactions of poly(dG-dC)·poly(dG-dC) with complex II of MTR and CHR demonstrated the importance of the sugars.[17] Footprinting studies with the antibiotic−DNA complexes showed that the two antibiotics exhibit differences in their sequence selectivity,[6,19] though the minimum requirement of two contiguous GC base pairs for association is conserved for both.[6] NMR studies indicated differences in geometry and orientation of the two antibiotics in their complexes with oligonucleotides such as d(TATGCATA)$_2$,[13,14] d(TTGGCCAA)$_2$,[15] and d(TCGCGA)$_2$.[18]

* Author to whom correspondence should be addressed: fax (091)-(033)-3374637; phone (091)-(033)-5565611; e-mail dipak@biop.saha.ernet.in.

† Saha Institute of Nuclear Physics.

‡ Present address: Chemistry Department, Lady Brabourne College, P1/2 Suhrawardy Ave., Kolkata 700 017, India.

§ Bose Institute.

|| Abbreviations: AUFS, absorbance unit full scale; au, arbitrary unit; CHR, chromomycin A_3; F_{540}, fluorescence emission intensity at 540 nm; Hepes, *N*-(2-hydroxyethyl)piperazine-*N*′-(2-ethanesulfonic acid); λ_{ex}, excitation wavelength; λ_{em}, emission wavelength; MTR, mithramycin; NMR, nuclear magnetic resonance; T_m, melting temperature; Tris, tris(hydroxymethyl)aminomethane.

10.1021/jp014710i CCC: $22.00
Published on Web 06/19/2002

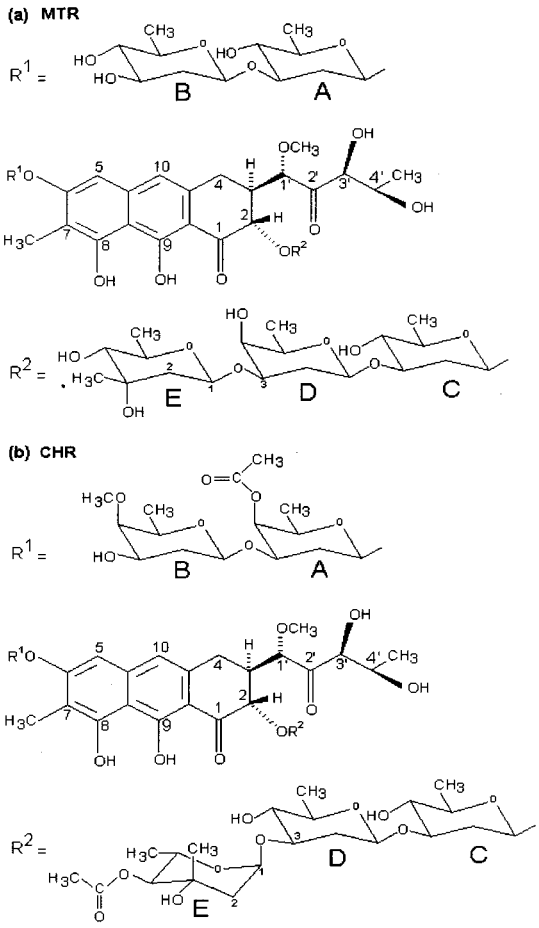

Figure 1. Structure of the antibiotics: (a) mithramycin and (b) chromomycin A_3.

As a part of the broad objective to understand the structural basis of DNA recognition by the two antibiotics, we have reported the roles of the minor-groove width and ligand flexibility, using GC-containing oligomers with progressive changes in minor-groove width.[20] In this report we have studied the association of the two (antibiotic)$_2$Mg^{2+} complexes with a model oligonucleotide, d(TAGCTAGCTA)$_2$, to understand the role of the sugar residues vis-a-vis ligand flexibility and subsequent DNA recognition.

We have examined the effects of sugars in the (antibiotic)$_2$Mg^{2+} upon ligand flexibility and concomitant DNA distortion during their association with DNA. The oligomer, d(TAGCTAGCTA)$_2$, is characterized by the presence of two GpC binding sites separated by one TpA step. Earlier reports of stoichiometry for complex II−DNA association has shown that the binding site per ligand molecule is around 5−6 bases in a random sequence like calf thymus DNA.[9,11] So there are two potential but partially overlapping binding sites in the oligomer. Such a sequence will be most suitable to compare the effects of the sugars upon binding potentials and geometry of complex II of the two antibiotics. Furthermore, complex II is preferred to complex I because (i) effects of sugar will be more apparent in the bulkier ligand and (ii) complex II is the species formed at the intracellular concentration of Mg^{2+}.[8,10]

Spectroscopic techniques such as absorbance and fluorescence have been used for the study because they permit us to work in the micromolar range of antibiotic concentration (10−50 μM), where aggregation of the free ligand is absent as detected by optical spectroscopic tools.[17] The interaction(s) have been characterized from spectroscopic studies and analysis of associated melting and thermodynamic parameters, obtained from van't Hoff analysis and calorimetric measurements. Results are compared with the structural information from a previous NMR study.[21]

Materials and Methods

Materials. Mithramycin, chromomycin A_3, Tris, and magnesium chloride solution (4.9 M) were from Sigma Chemical Co. The oligomer d(TAGCTAGCTA)$_2$ was synthesized on a Gene Assembler Special instrument from Pharmacia Biotech Ltd., Sweden, by the phosphoramidite method. Its purity was checked from a single band in 20% native polyacrylamide gel electrophoresis and a single peak in reverse-phase HPLC column chromatography on a ProRPC HR 5/10 column. Concentrations of the antibiotics were determined from their known molar extinction coefficients.[8,9] Concentration of the oligomer was determined from extinction coefficient values calculated by phosphate estimation.[22] Buffers used were 20 mM Tris-HCl buffer plus 10 mM $MgCl_2$, pH 8.0, for binding studies and 5 mM Hepes buffer plus 10 mM $MgCl_2$, pH 8.0, for UV DNA melting experiments. They were prepared in deionized, all-quartz-distilled water.

Binding Studies. The antibiotic was incubated with 10 mM Mg^{2+} for 1 h [corresponding to 8 half-life periods for formation of (antibiotic)$_2$Mg^{2+} complex[8,10]] at the desired temperature to ensure complete formation of (antibiotic)$_2$Mg^{2+} complex. A small aliquot of oligomer was then added to the complex and the spectrum was recorded after equilibration. Absorbance and fluorescence spectra were recorded on a Hitachi U-2000 spectrophotometer and a Shimadzu RF-540 spectrofluorometer, respectively. For fluorescence measurements, the antibiotics were excited at 470 nm instead of their absorbance maxima to avoid photodegradation.[8] Absorbance of the samples at 470 nm did not exceed 0.02. Therefore, we did not correct the emission intensity for the optical filtering effect. Background emission (<5% of maximum) was corrected for by subtracting signals from blank buffer.

UV Melting Studies. Ultraviolet DNA melting curves were determined on a Hitachi U-3300 spectrophotometer, equipped with a programmable thermoelectric temperature controller. Oligonucleotide samples preincubated with 10 mM $MgCl_2$ were used for the study in 5 mM Hepes buffer plus 10 mM $MgCl_2$, pH 8.0. To a final concentration of 100 μM of the oligomer was added 40 μM (in terms of antibiotic) complex II, to ensure saturation of the DNA molecule with the ligand. The samples were then further incubated for 30 min for equilibrium to be established. During melting experiments the samples were heated rapidly till 26 °C at the rate of 3 °C/min. Further heating was carried out slowly, at the rate of 1 °C/min, while the absorbance was continuously monitored at 260 nm. Reversibility of the melting profile was checked by slow cooling of the melted sample. The resulting annealing curve overlaps the melting curve. Spectrum of the oligomer-bound ligand(s) before melting also remains unaltered after the cooling cycle, thereby indicating thermal stability of the antibiotic(s).

Analysis of Binding Data. All spectrophotometric and spectrofluorometric titrations were carried out at least 20 °C below the melting temperature of the oligomer. Results from spectrophotometric and spectrofluorometric titrations were analyzed by the following methods. Apparent binding constant ($K_{ap} = 1/K_d$) was determined by nonlinear curve-fitting analysis

based on the equilibrium L + P ⇌ L−P, where

$$K_d = [L][P]/[L-P] = \{[L]_0 - [L-P]\}\cdot\{[P]_0 - [L-P]\}/[L-P]$$

In the above equation L, P, and L−P denote ligand, DNA, and ligand−DNA complex, respectively. Subscript 0 denotes the input concentration for each of them. Spectrofluorometric data were analyzed by eqs 1 and 2. Spectrophotometric data were analyzed by means of eqs 3 and 4. All experimental points for binding isotherms were fitted by least-squares analysis.

$$K_d = [C_0 - (\Delta F/\Delta F_{max})C_0][C_p - (\Delta F/\Delta F_{max})C_0]/[(\Delta F/\Delta F_{max})C_0] \quad (1)$$

$$C_0(\Delta F/\Delta F_{max})^2 - (C_0 + C_p + K_d)(\Delta F/\Delta F_{max}) + C_p = 0 \quad (2)$$

$$K_d = [C_0 - (\Delta A/\Delta A_{max})C_0][C_p - (\Delta A/\Delta A_{max})C_0]/[(\Delta A/\Delta A_{max})C_0] \quad (3)$$

$$C_0(\Delta A/\Delta A_{max})^2 - (C_0 + C_p + K_d)(\Delta A/\Delta A_{max}) + C_p = 0 \quad (4)$$

where ΔF is the change in fluorescence emission intensity at 540 nm ($\lambda_{ex} = 470$ nm) for each point of titration curve, ΔF_{max} is the same parameter when the ligand is totally bound to oligomer, C_p is the concentration of the oligomer, and C_0 is the initial concentration of the antibiotic. ΔA is the increase in absorbance (at 450 nm) of the ligand upon each addition of the oligonucleotide; ΔA_{max} is the same parameter when the ligand is totally bound to oligomer. In the above equations 1−4, the terms $\Delta F/\Delta F_{max}$ and $\Delta A/\Delta A_{max}$ denote the fraction of ligand bound to DNA. A double-reciprocal plot of $1/\Delta F$ (or $1/\Delta\epsilon$) against $1/(C_p - C_0)$ was used for determination of ΔF_{max} and ΔA_{max} by use of eqs 5[23] and 6,[24] respectively. $\Delta A_{max} = \Delta\epsilon'/C_0$ for 1.0 cm optical path length.

$$1/\Delta F = 1/\Delta F_{max} + 1/[K_{ap}\Delta F_{max}(C_p - C_0)] \quad (5)$$

$$1/\Delta\epsilon = 1/\Delta\epsilon' + 1/[K_{ap}\Delta\epsilon'(C_p - C_0)] \quad (6)$$

$\Delta\epsilon = \epsilon_{obs} - \epsilon_f$, where ϵ_{obs} is the apparent molar extinction coefficient of the bound ligand measured from the observed absorbance for each point in the titration curve and ϵ_f is the molar extinction coefficient of the free ligand, and $\Delta\epsilon' = \epsilon_b - \epsilon_f$ (ϵ_b is the molar extinction coefficient of the bound ligand). The approach is based on the assumption that spectroscopic signal (both absorbance and emission intensity) is linearly proportional to the concentration of the ligand, which is found to be true for the concentration range of 10−50 μM of the ligands employed and under the condition $C_p \gg C_0$, which was followed by keeping at least 8-fold excess of oligomer with respect to antibiotic concentration.

The second method uses the Scatchard equation to estimate the intrinsic binding constant (K_0), binding stoichiometry ($1/n$), and K_{ap} ($= K_0 n$):

$$r/C_f = K_0(n - r) \quad (7)$$

r/C_f was plotted against r and the best-fit straight line of the experimental points was drawn. In the above equation, $r = C_b/C_p$, where C_b is the concentration of the bound ligand and C_p is the concentration of oligomer. The concentration of the bound ligand was determined from fluorometric titration by use of the expression $C_b = (\Delta F/\Delta F_{max})C_0$.

Evaluation of Binding Stoichiometry. The method of continuous variation provides a reliable way to determine DNA−antibiotic binding stoichiometry. At constant temperature, the fluorescence signal was recorded for solutions where the concentrations of both oligomeric duplex and ligand are varied while the sum of their concentrations was kept constant.[25] F_{540} was plotted as a function of the input mole fraction of ligand, χ_{ligand} (= molar concentration of ligand/total molar concentration of ligand and oligomeric duplex). The break point in the resulting plot corresponds to the mole fraction of ligand in the complex with oligomeric duplex. Therefore, stoichiometry is obtained in terms of ligand:duplex [χ_{ligand}:(1 − χ_{ligand})]. These were done at three temperatures of 15, 20, and 25 °C.

Binding stoichiometry in terms of nucleotide bases per antibiotic was determined from the intersection of the two straight lines in the plot of normalized increase in fluorescence against the ratio of the input concentrations of the oligomer and antibiotic. Binding stoichiometry obtained from a Scatchard plot is also in terms of the number of nucleotide bases bound per molecule of antibiotic.

Evaluation of Thermodynamic Parameters. Thermodynamic parameters ΔH (van't Hoff enthalpy), ΔS (entropy), and ΔG (free energy) were determined from[26]

$$\ln K_{ap} \text{ (or } K_0) = -\Delta H/RT + \Delta S/R \quad (8)$$

$$\Delta G = \Delta H - T\Delta S \quad (9)$$

where R and T are the universal gas constant and absolute temperature, respectively. K_{ap} (or K_0) was determined at 15, 20, and 25 °C to evaluate ΔH and ΔS. These values were incorporated in eq 9 to obtain the value of ΔG. van't Hoff ΔH values for the association were also calculated from the DNA melting curves. Enthalpy changes (ΔH) for the following equilibria were considered as sum of two parts according to earlier reports:[27,28]

$$2 \text{ single strands} \rightleftharpoons \text{duplex } [\Delta H_1]$$

$$(\text{antibiotic})_2Mg^{2+} + 2 \text{ single strands} \rightleftharpoons (\text{antibiotic})_2Mg^{2+} - \text{duplex } [\Delta H_2]$$

By combination of these two reactions, the binding reaction and its ΔH_3 may be obtained:

$$(\text{antibiotic})_2Mg^{2+} + \text{duplex} \rightleftharpoons (\text{antibiotic})_2Mg^{2+} - \text{duplex } [\Delta H_3 = \Delta H_2 - \Delta H_1]$$

ΔH_1 and ΔH_2 were determined from[29]

$$\Delta H = -4.38/[(1/T_{max}) - (1/T)] \quad (10)$$

where T_{max} is the temperature at the peak and T is the temperature corresponding to the half-height of the peak on the higher temperature side in the differential melting curve.

Isothermal titration calorimetry (ITC) was also used to obtain the values of enthalpy change during antibiotic−oligomer interactions at two temperatures, 15 and 25 °C. A VP-ITC MicroCalorimeter from Microcal Inc. was used for the purpose. Data were analyzed with MicroCal Origin Version 5.0. A single shot of 270 μL of the ligand (500 μM) was injected into the sample cell containing the oligomer (100 μM), leading to a final molar ratio of 1. The heat change corresponding to the

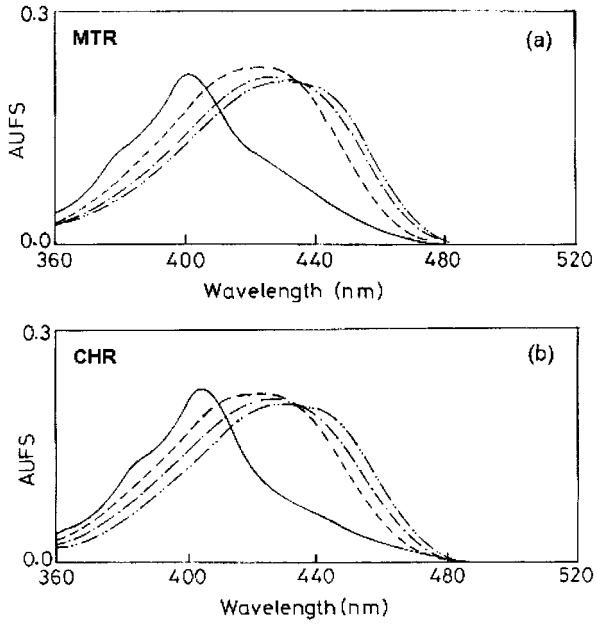

Figure 2. Absorbance spectra (360−520 nm) of the antibiotics under different conditions in 20 mM Tris-HCl, pH 8.0 at 25 °C. (a) MTR alone ([MTR] = 20 μM, —); complex II ([MTR] = 20 μM, [Mg^{2+}] = 10 mM, ---); complex II in the presence of d(TAGCTAGCTA)$_2$ (98 μM, — · —, and 387 μM, — ·· —). (b) CHR alone ([CHR] = 20 μM, —); complex II ([CHR] = 20 μM, [Mg^{2+}] = 10 mM, ---); complex II in the presence of d(TAGCTAGCTA)$_2$ (149 μM, — · —, and 534 μM, — ·· —).

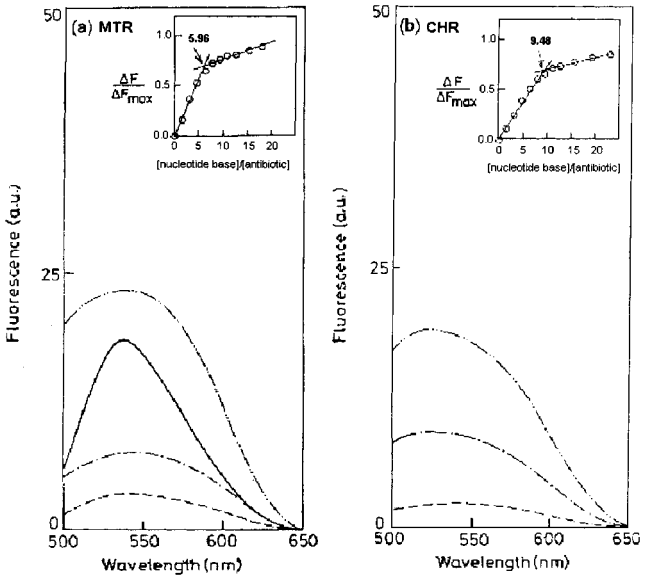

Figure 3. Fluorescence emission spectra (500−650 nm) of the antibiotics (λ_{ex} = 470 nm) under different conditions in 20 mM Tris-HCl, pH 8.0 at 25 °C. (a) MTR alone ([MTR] = 20 μM, —); complex II ([MTR] = 20 μM, [Mg^{2+}] = 10 mM, ---); complex II in the presence of d(TAGCTAGCTA)$_2$ (33 μM, — · —, and 255 μM, — ·· —). **(b)** Complex II ([CHR] = 20 μM, [Mg^{2+}] = 10 mM, ---); complex II in the presence of d(TAGCTAGCTA)$_2$ (68 μM, — · —, and 390 μM, — · · —). Insets represent binding isotherms for respective ligands with d(TAGCTAGCTA)$_2$. Normalized increase in fluorescence ($\Delta F/\Delta F_{max}$) is plotted against ratio of molar concentrations of nucleotide base and antibiotic. ΔF denotes change in fluorescence emission intensity (λ_{em} = 540 nm) after each addition of each aliquot of oligomer to the ligand, and ΔF_{max} denotes maximum value of the same. Excitation and emission band-passes were 5 and 10 nm, respectively. Stoichiometry in terms of number of nucleotide bases/antibiotic molecule is obtained from the point of intersection of the two straight lines.

association process was obtained from area under the curve after appropriately subtracting the heat of dilution for the ligand.

Results

Association of complex II of MTR and CHR with d(TAGCTAGCTA)$_2$ is indicated from spectral changes of the free ligand upon addition of the oligonucleotide. Red shift and broadening of the absorbance peak in the visible region (Figure 2) marks the association. In each case, there is also a concomitant increase in absorbance in the higher wavelength range, the extent of which is dependent on the nature of the ligand. The presence of an isosbestic point supports analysis in terms of free ligand and a single type of bound species. Association with the oligomer also increases the fluorescence emission intensity of the ligand(s) along with a blue shift of the peak (Figure 3). The peak shifts by about 8 nm for the association of $(MTR)_2Mg^{2+}$ and by 20 nm for the association of $(CHR)_2Mg^{2+}$. Extent of increase in the fluorescence quantum yield upon association with the oligomer is also dependent on the nature of the ligand. Insets to Figure 3 represent corresponding binding isotherms. Each isotherm has been fitted to two straight lines that yield the value of binding stoichiometry from the point of intersection. Binding stoichiometry (obtained in terms of number of nucleotide bases bound per molecule of the antibiotic) is different for MTR and CHR. This might originate from a difference in the modes of recognition of the same DNA sequence by the two ligands. Since the binding stoichiometry values are markedly different, we evaluated them by the direct method of continuous variation. The representative results are shown in Figure 4a. In the case of MTR, an inflection point appears at $\chi_{ligand} = 0.66$, from which a mole ratio of 1.94 (= 0.66/0.34) is obtained for ligand:duplex. This implies that two molecules of $(MTR)_2Mg^{2+}$ bind the duplex. In the case of CHR, an inflection point is at $\chi_{ligand} = 0.49$, which yields a ligand:duplex mole ratio of 0.96 (= 0.49/0.51). Here, one molecule of $(CHR)_2Mg^{2+}$ binds per duplex. These results corroborate the trend shown in the insets of Figure 3.

Binding parameters for the association of complex II with d(TAGCTAGCTA)$_2$ were also determined from absorbance and fluorescence titrations. Apparent binding constant values were estimated by nonlinear curve-fitting analysis as shown in Figure 4b for CHR. Both binding constants and binding stoichiometry were also obtained from Scatchard plots. Scatchard plots show dispersion of some points from the fitted linear equation. In most cases we get a good fit with a correlation coefficient above 0.8, with a confidence level of >99%. Representative examples are shown in Figure 4c, for which the statistical binding parameters are indicated in Table 1. Comparison of these parameters shows that there is a difference in the binding of the two ligands with the decameric sequence. The binding stoichiometry is ∼5 nucleotide bases/molecule of MTR as compared to ∼10 bases/molecule of CHR. Results from three different approaches to determine stoichiometry show internal consistency. It indicates that $(MTR)_2Mg^{2+}$ binds to both potential sites (GpC) in the decamer. In contrast, $(CHR)_2Mg^{2+}$ complex binds only to a single site.

Thermodynamic parameters of association were determined from van't Hoff plots of variation of affinity constants (both K_{ap} and K_0) with temperature (Figure 5a, Table 2). Both interactions were found to be exothermic in nature. Enthalpy changes for the interaction of $(CHR)_2Mg^{2+}$ with the decamer at two different temperatures of 15 and 25 °C were also determined by isothermal calorimetry (Figure 5b). It is important to note that the values at two temperatures are consistent with

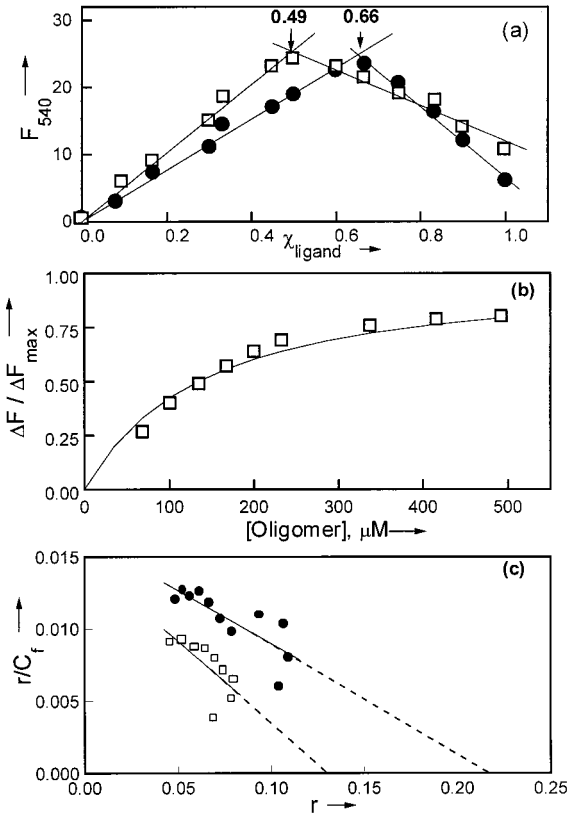

Figure 4. Analysis of binding for association of the antibiotics with d(TAGCTAGCTA)$_2$ in 20 mM Tris-HCl buffer plus 10 mM $MgCl_2$, pH 8.0. (a) Continuous variation plot for the interaction of $(MTR)_2Mg^{2+}$ (●) and $(CHR)_2Mg^{2+}$ (□) with the oligomer at 25 °C. Fixed concentration sum for ligand and duplex is 18 μM. Mole fractions (χ) have been calculated in terms of concentration of total ligand [$(antibiotic)_2Mg^{2+}$] or oligomeric duplex (20 bases/molecule). F_{540} (λ_{ex} = 470 nm) is the emission intensity for different mole fractions of ligand with duplex. Two straight lines are fitted by least-squares analysis. (b) Spectrofluorometric titration of $(CHR)_2Mg^{2+}$ (□) at 25 °C. ΔF denotes the change in fluorescence emission intensity (λ_{ex} = 470 nm, λ_{em} = 540 nm) after each addition of oligomer to the ligand, and ΔF_{max} denotes the maximum value of the same. Best curve is generated by nonlinear fitting of experimental points. (c) Scatchard plot for interaction of $(MTR)_2Mg^{2+}$ (●) and $(CHR)_2Mg^{2+}$ (□) with the decamer at 25 °C, determined from spectrofluorometric titration.

each other, thereby supporting the linear nature of the van't Hoff plot (Figure 5a). Furthermore, the values obtained from van't Hoff and calorimetric methods agree well with each other (Table 2). High heat of dilution for MTR prevented us from estimating enthalpy change for $(MTR)_2Mg^{2+}$−oligomer association by the calorimetric method.

DNA melting experiments further illustrate the differential nature of interaction between the two antibiotics with the same oligomer. Panels a and b of Figure 6 show the normalized melting profiles and the corresponding differential curves, respectively, for the oligomer in the presence and absence of saturating concentrations of the two ligands. To determine the melting curves for the ligand-bound oligomers, the amount of ligand added was so adjusted that the oligomer is completely saturated, and there exists only a single species of ligand-bound oligomer in the sample. The oligomer was preincubated with 10 mM $MgCl_2$ to maintain the same condition in which the binding studies were carried out. Melting temperatures (T_m) were determined from the corresponding differential melting profiles (Figure 6b). The oligomeric duplex in the absence of ligand(s) melts symmetrically with T_m at 45 °C. It is stabilized upon association with $(MTR)_2Mg^{2+}$; T_m shifts to 56 °C. However, in

TABLE 1: Binding Parameters for the Association of Complex II[a] with d(TAGCTAGCTA)$_2$

antibiotic	$K_{ap} \times 10^{4\,b}$ (M^{-1})	$K_0 \times 10^{5\,c}$ (M^{-1})	stoichiometry[d]	R[e]
MTR	0.9	0.7	4.9 ± 0.1	0.81
	(1.6)		(6.4 ± 0.5)	(>99%)
CHR	0.8	1.1	8.3 ± 0.5	0.70
	(0.5)		(9.8 ± 0.6)	(98%)

[a] Complex II was prepared by incubating 20 μM of the antibiotic(s) with 10 mM $MgCl_2$ for 1 h in the dark to ensure complete complex formation. The complex was incubated with oligomer in 20 mM Tris-HCl buffer, pH 8.0, at 25 °C to determine binding parameters [b] Apparent binding constants are determined from spectrofluorometric data by nonlinear curve-fitting analysis. Values in parentheses were determined from spectrophotometric data. [c] Intrinsic binding constants are determined from spectrofluorometric data by Scatchard plots. [d] Binding stoichiometry in terms of number of nucleotide bases bound per antibiotic molecule is reported from a Scatchard plot. Values in parentheses are determined from point of intersection of the two straight lines fitted to a plot of normalized increase in fluorescence against the ratio of molar concentration of the oligomer to antibiotic as described under Materials and Methods. Stoichiometry reported is determined from four independent sets of experiments. [e] Correlation coefficients for the data fitted to linear Scatchard equations are reported, and values in parentheses denote the corresponding confidence level of fitted data.

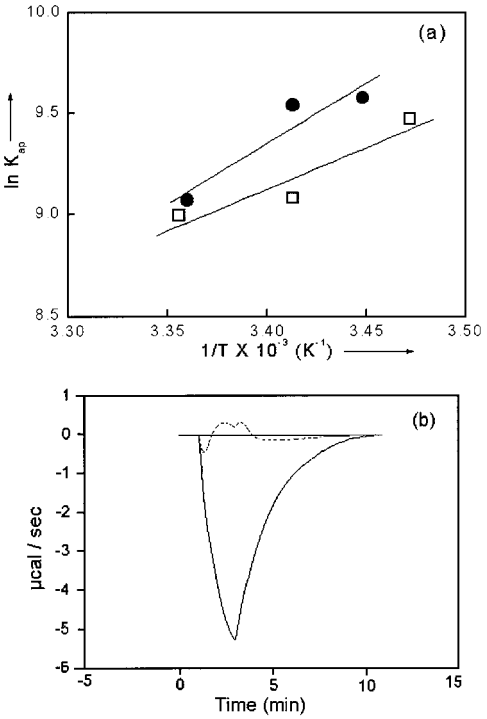

Figure 5. Estimation of thermodynamic parameters for association of antibiotics with d(TAGCTAGCTA)$_2$ in 20 mM Tris-HCl buffer plus 10 mM $MgCl_2$, pH 8.0. (a) van't Hoff plot for the interaction of $(MTR)_2Mg^{2+}$ (●) and $(CHR)_2Mg^{2+}$ (□) with the decamer. (b) Isothermal calorimetry for $(CHR)_2Mg^{2+}$ with the decamer: a single shot of ligand was injected to oligomeric duplex (100 μM), leading to a final molar ratio of 1. Dotted curve denotes the heat change corresponding to dilution of the ligand in the same buffer.

the case of saturation with $(CHR)_2Mg^{2+}$, the single peak in the differential curve is replaced by two distinct peaks separated by 12 °C. The lower peak is at 37 °C, less than the T_m value for the free oligomer (45 °C). The second peak is at 49 °C (Figure 6). In general, melting of a single DNA molecule with two distinct T_m values is caused by significant differences in the duplex stability at two different regions in the sequence. The presence of distinct AT- and GC-rich sequences in different regions of a DNA molecule can also give rise to more than a

TABLE 2: Thermodynamic Parameters for the Association of Complex II with the Oligomer d(TAGCTAGCTA)$_2$

antibiotic	ΔG^a (kcal/mol)	ΔS^b (eu)	$\Delta H^{b,c}$ (kcal/mol)	ΔH^d (kcal/mol)
MTR	−5.4	−33.6 ± 11.8	−15.4 ± 3.5	−15.0
CHR	−5.3	−18.0 ± 8.3	−10.3 ± 2.5 (−9.2 ± 1.4)	−12.1

[a] The value for ΔG is stated at 25 °C. [b] The values are determined from van't Hoff plots. ΔH and ΔS values have been obtained from variation of K_{ap} (from nonlinear curve-fitting analysis) and K_0 (from the Scatchard equation) as a function of temperature, according to eq 8, and the mean of the two values is reported. Binding constants have been calculated from fluorometric titration data. [c] ΔH value in parentheses is obtained from two isothermal microcalorimetric measurements at 15 and 25 °C. [d] The values are obtained from the oligomer melting profile by use of eq 10 as described under Materials and Methods.

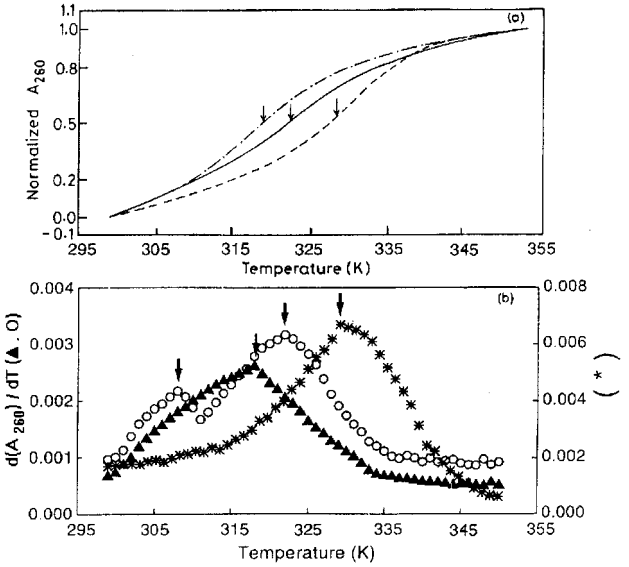

Figure 6. Ultraviolet DNA melting curves for d(TAGCTAGCTA)$_2$ in 5 mM Hepes buffer plus 10 mM $MgCl_2$, pH 8.0, under different conditions. (a) Normalized value of absorbance at 260 nm (A_{260}) plotted as a function of temperature for the following systems: free oligomer (100 μM, −·−), oligomer saturated with $(MTR)_2Mg^{2+}$ complex ([nucleotide base]/[MTR] = 2.5, ---), and oligomer saturated with $(CHR)_2Mg^{2+}$ ([nucleotide base]/[CHR] = 2.5, —). (b) Derivative of absorbance with respect to temperature [$d(A_{260})/dT$] plotted as a function of temperature for the following systems: free oligomer (100 μM, ▲), oligomer saturated with $(MTR)_2Mg^{2+}$ ([nucleotide base]/[MTR] = 2.5, *), and oligomer saturated with $(CHR)_2Mg^{2+}$ ([nucleotide base]/[CHR] = 2.5, O).

single peak in the differential melting curve.[28] Here, preferential stabilization of one part of the duplex originating from asymmetric association of CHR with a single binding site is the plausible reason for the appearance of two peaks.

Binding enthalpy for the antibiotic−oligomer interactions was also calculated from the differential DNA melting curves as described under Materials and Methods. In the case of $(CHR)_2Mg^{2+}$, the enthalpy change was calculated from the peak at the higher temperature on the assumption that it relates to the ligand-bound site. The values are included in Table 2. In the case of $(CHR)_2Mg^{2+}$, ΔH values from van't Hoff plots, melting curves, and calorimetric methods are consistent within the limits of experimental error, thereby validating the application of the methods to understand the mode of association. The agreement between the two sets of values in the case of $(MTR)_2Mg^{2+}$, where clean calorimetry could not be done, also supports the above assumption. Table 2 shows that the negative values of ΔH are higher for association of $(MTR)_2Mg^{2+}$ as compared to $(CHR)_2Mg^{2+}$. A similar trend characterizes the accompanying negative value of ΔS.

Discussion

We have reported here the interaction of complex II of MTR and CHR with the decameric sequence d(TAGCTAGCTA)$_2$. Absorbance and fluorescence spectra for the two oligomer-bound ligands have specific dissimilarities between them (Figures 2 and 3). This could arise from a difference in (i) electronic environment of the ligands in the complexes and/or (ii) conformation of antibiotic in $(antibiotic)_2Mg^{2+}$ molecule. Table 1 shows the internal consistency of the values for binding parameters obtained from analysis of titration data based on model-dependent (Scatchard plot) and independent (nonlinear curve-fitting) approaches. Agreement of the values from spectrophotometric and fluorescence data further lends support to the methods of measurement. Apparent binding constants for the two antibiotics are comparable at 25 °C. However, binding stoichiometry between the ligand and oligomeric duplex is the more relevant parameter in the present context to characterize the binding modes. That is why we took three different approaches to estimate its value. In terms of the ligand:duplex concentration, it is 2:1 for $(MTR)_2Mg^{2+}$ and 1:1 for $(CHR)_2Mg^{2+}$, respectively (Figures 3 and 4a,c). Association of $(CHR)_2Mg^{2+}$ with one of the binding sites in the decamer leads to its asymmetric melting at two different temperatures (Figure 6). Summing up, the above observations suggest that the two $(antibiotic)_2Mg^{2+}$ ligands bind differently to the same oligomeric DNA. In the following section, we have correlated this difference with structures of the two antibiotics, particularly in terms of their sugar moieties.

Comparison of the binding stoichiometry for the association of $(MTR)_2Mg^{2+}$ and $(CHR)_2Mg^{2+}$ with the decamer implies that, in the $(MTR)_2Mg^{2+}$−oligomer complex, both sites are occupied. On the other hand, in the $(CHR)_2Mg^{2+}$−oligomer complex, only one of the two potential binding sites (GpC) in the oligomer is bound to the ligand. Binding stoichiometry reported from a relevant NMR study on the interaction of $(MTR)_2Mg^{2+}$ complex with the oligomer also proposed a 2:1 stoichiometry,[21] which is consistent with the present report. NMR data have shown that the DNA molecule gets kinked at the intermediate TpA step, resulting in significant curvature of the decamer and its opening toward the minor groove, which is widened from a B- to an A-type minor groove. This leads to generation of additional space for the approach, leading to an accommodation of two bulky $(MTR)_2Mg^{2+}$ ligands. The ligand molecules also undergo significant conformational alteration in order to fit into the groove without steric clash between them. The conformational alteration involve changes in the glycosidic linkage bonds in the C-D-E trisaccharide in one of the monomers of the $(MTR)_2Mg^{2+}$ ligand.

Analysis of thermodynamic parameters and results from melting studies further support difference in the binding modes of the two $(antibiotic)_2Mg^{2+}$ ligands with the oligomer. We have discussed these aspects in the light of the two different structures of the antibiotics. As in our earlier reports, we have analyzed the observed change in enthalpy as a sum of several contributing terms[17] in the following manner:

$$\Delta H_{tot} = \Delta H_{bind} + \Delta H_{DNA} + \Delta H_{dimer}$$

where ΔH_{bind} is the binding enthalpy and ΔH_{DNA} and ΔH_{dimer} are the enthalpy changes associated with structural alterations in the DNA molecule and the ligand molecule, respectively,

during their interaction. The comparative ΔH values show that binding in the case of $(MTR)_2Mg^{2+}$ involves a higher enthalpy change (Table 2). It is not twice the value observed for $(CHR)_2Mg^{2+}$, even though two $(MTR)_2Mg^{2+}$ molecules interact with the oligomer. This can be attributed to the positive enthalpy change arising out of ligand-induced alterations in oligomer conformation like (i) kinking of the decamer at the TpA step leading to (ii) an opening up of the minor groove from a B- → A-type structure, as proposed in the NMR spectroscopy-based model (vide PDB ID 207d[21,30]). The higher negative value of ΔS for $(MTR)_2Mg^{2+}$ also occurs due to structural distortions of ligand and oligomer that decrease their conformational flexibility. A notable feature is that ΔG values remain comparable for both types of ligands due to enthalpy−entropy compensation.

The difference in the energetics of the ligand−oligomer interaction originates from the substituents present in the A, B, and E sugars, where CHR and MTR differ structurally. In contrast to MTR, the methoxy group present in the B sugar and acetoxy groups in the A and E sugars of CHR impose constraints upon the free rotations about the glycosidic linkages in the disaccharide and trisaccharide chains in the ligand, $(CHR)_2Mg^{2+}$. Energetically permissible structural changes in the ligand molecule, such as alterations in the glycosidic torsion angles of the C-D-E trisaccharide segment, may be absent in the case of CHR. It reduces the flexibility of the $(CHR)_2Mg^{2+}$ ligand, making it relatively more rigid with respect to $(MTR)_2Mg^{2+}$. This is also supported from our earlier reports that the DNA-bound conformation of the $(CHR)_2Mg^{2+}$ ligand is more sensitive to groove dimension as compared to $(MTR)_2Mg^{2+}$.[17,20]

Differences in the nature of the ligand−DNA complexes formed by the two antibiotics is also reflected in the melting profiles of the oligomer in ligand−oligomer complexes. The melting profile for the conformationally flexible $(MTR)_2Mg^{2+}$-bound decamer is characterized by a single peak, because the ligand binds and stabilizes both sites. On the other hand, the asymmetric association of $(CHR)_2Mg^{2+}$ with 1:1 stoichiometry gives rise to two distinct peaks. The GpC site, where the $(CHR)_2Mg^{2+}$ ligand binds, is stabilized. Due to the rigidity of the ligand, its association with the oligomer necessitates a considerable extent of DNA distortion, both at the binding site and also around it. This leads to partial unwinding and significant destabilization of the second GpC site once the first site is occupied. A lower T_m as compared to that of the free duplex (Figure 6) occurs as a sequel to this destabilization. The second site is thus structurally unfit for interaction with a second $(CHR)_2Mg^{2+}$ ligand. The proposed mode of interaction of $(CHR)_2Mg^{2+}$ with the oligomer is represented schematically in Figure 7.

Differences in the extent of DNA distortion induced by $(MTR)_2Mg^{2+}$ and $(CHR)_2Mg^{2+}$ ligands were also earlier reported by us from a study of their interactions with polymeric DNA.[17] We showed that acetoxy groups (in the A and E sugars of CHR) with hydrogen-bonding ability could be a potential source for difference in the DNA recognition properties of the antibiotics. The present work has shown that conformational flexibility in the saccharides of the antibiotics plays an important role in the DNA recognition process. Together, these two results elucidate the structural roles of the sugars in the antibiotic−DNA recognition.

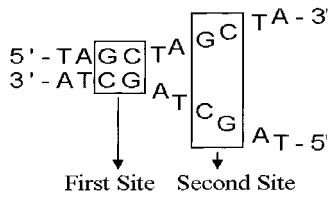

Figure 7. Schematic model for the asymmetric association of $(CHR)_2Mg^{2+}$ with oligomer $d(TAGCTAGCTA)_2$.

Acknowledgment. S.C. thanks Professor (Dr.) B. Sinha, Director of SINP, for his permission to allow her to work in the Biophysics Division as a part of her Ph.D. program. Authors acknowledge the technical assistance of Asim Poddar, Biochemistry Department, Bose Institute, to run the calorimeter.

References and Notes

(1) Rohr, J.; Mendez, C.; Salas, J. A. *Bioorg. Chem.* **1999**, *27*, 41.
(2) Gause, G. F. In *Antibiotics III*; Corocan, J. W., Hahn, F. E., Eds.; Springer-Verlag: Berlin and New York, 1975; p 197.
(3) Chabner, B. A.; Allegra, C. J.; Curt, G. A.; Calabresi, P. In *Goodman & Gilman's The Pharmacological Basis of Therapeutics*, 9th ed.; Hardman, J. G., Limbird, L. E., Molinoff, P. B., Ruddon, R. W., Gilman, A. G., Eds.; McGraw-Hill: New York, 1996; p 1233.
(4) Goldberg, I. H.; Friedman, P. A. *Annu. Rev. Biochem.* **1971**, *40*, 775.
(5) Waring, M. J. *Annu. Rev. Biochem.* **1981**, *50*, 159.
(6) van Dyke, M. W.; Dervan, P. B. *Biochemistry* **1983**, *22*, 2373.
(7) Stankus, A.; Goodisman, J.; Dabrowiak, J. C. *Biochemistry* **1992**, *31*, 9310.
(8) Aich, P.; Dasgupta, D. *Biochem. Biophys. Res. Commun.* **1990**, *173*, 689.
(9) Aich, P.; Sen, R.; Dasgupta, D. *Biochemistry* **1992**, *31*, 2988.
(10) Aich, P.; Sen, R.; Dasgupta D. *Chem.-Biol. Interact.* **1992**, *83*, 23.
(11) Aich, P.; Dasgupta, D. *Biochemistry* **1995**, *34*, 1376.
(12) Chakrabarti, S.; Mir, M. A.; Dasgupta, D. *Biopolymers* **2001**, *62*, 131.
(13) Banville, D. L.; Keniry, M. A.; Shafer, R. H. *Biochemistry* **1990**, *29*, 6521.
(14) Banville, D. L.; Keniry, M. A.; Shafer, R. H. *Biochemistry* **1990**, *29*, 9294.
(15) Gao, X.; Patel, D. J. *Biochemistry* **1989**, *28*, 751.
(16) Illarivova, R. P.; Dykhovichnaya, D. E.; Bondarenko, B. N. *Antibiotiki (Moscow)* **1970**, *15*, 415 (in Russian).
(17) Majee, S.; Sen, R.; Guha, S.; Bhattacharyya, D.; Dasgupta, D. *Biochemistry* **1997**, *36*, 2291.
(18) Sastry, M.; Patel, D. J. *Biochemistry* **1993**, *32*, 6588.
(19) Fox, K. R.; Howarth, N. R. *Nucleic Acids Res.* **1985**, *13*, 8695.
(20) Chakrabarti, S.; Bhattacharyya, D.; Dasgupta, D. *Biopolymers* **2000−2001**, *56*, 85.
(21) Sastry, M.; Fiala, R.; Patel, D. J. *J. Mol. Biol.* **1995**, *251*, 674.
(22) Muraoka, M.; Miles, T. H.; Howard, F. B. *Biochemistry* **1980**, *19*, 2429.
(23) Wang, J. L.; Edelman, G. H. *J. Biol. Chem.* **1971**, *246*, 1185.
(24) Dasgupta, D.; Goldberg, I. H. *Biochemistry* **1985**, *24*, 6913.
(25) Jenkins, T. C. *Methods Mol. Biol.* **1997**, *90*, 195.
(26) Castellan, G. W. *Physical Chemistry*, 3rd ed.; Addison-Wesley/Narosa Publishing House (Indian student edition): New Delhi, 1989; p 221.
(27) Chaires, B. C.; Leng, F.; Przewloka, T.; Fokt, I.; Ling,Y. H.; Perez-Soler, R.; Priebe, W. *J. Med. Chem.* **1997**, *40*, 261.
(28) Leng, F.; Priebe, W.; Chaires, J. B. *Biochemistry* **1998**, *37*, 1743.
(29) Marky, L. A.; Breslauer, K. J. *Biopolymers* **1987**, *26*, 1601.
(30) Berman, H. M.; Westbrook, J.; Feng, Z.; Gilliland, G.; Bhat, T. N.; Weissig, H.; Shindyalov, I. N.; Bourne. P. E. *Nucleic Acids Res.* **2000**, *28*, 235.